

# Geometrical Self-Calibration of CBCT Systems

Amirhossein Saedpanah<sup>1,2</sup>, Seyed Mohammad Hosseini<sup>3</sup>, Seyed Roohollah Hosseini<sup>1,4\*</sup>, Abbas Mohammadkazemi<sup>1,5</sup>

<sup>1</sup> Arman Moj Fanavar Co., Tehran, Iran

<sup>2</sup> Department of physics, Sharif university of technology, Tehran, Iran, e-mail: [Amirhossein.saedpanah@gmail.com](mailto:Amirhossein.saedpanah@gmail.com)

<sup>3</sup> Electrical Engineering Department, university of Tehran, Tehran, Iran, e-mail: [mohammad.hussini@ut.ac.ir](mailto:mohammad.hussini@ut.ac.ir)

<sup>4</sup> Department of physics, University of Tehran, Tehran, Iran, e-mail: [sr\\_hosseini@ut.ac.ir](mailto:sr_hosseini@ut.ac.ir)

<sup>5</sup> Department of physics, University of Qom, Qom, Iran, e-mail: [a.m.kazemi@gmail.com](mailto:a.m.kazemi@gmail.com)

## Abstract

In this paper, we intend to provide a method for calibration of geometric CBCT systems without the need for phantom and prior knowledge related to the object which is normally used in 2D-3D registration methods for geometrical calibration. To this end, we use an iterative algorithm based on comparison between measured data and DRRs<sup>1</sup> which are obtained from reconstructed images with different geometries to find geometrical parameters of the system. Our proposed method shows strong agreement with phantom based methods.

**Keywords:** Geometrical Calibration, CT-scan, Self-Calibration, Optimization, Gradient Descent, Mutual-Information

## 1 introduction

Today, CT-scan is used as a powerful tool for non-destructive testing and metrology in many industries. In CT imaging, the quality of the reconstructed images is highly dependent on the determination of geometric parameters of the system. Incorrect parameters will degrade image qualities such as degeneration of the resolution, more artefacts in the images, and so on. Thus, the geometric parameters must be carefully calibrated and correctly involved in the reconstruction algorithms.

Recently, many calibration approaches have been proposed to acquire the geometric parameters of CT-scan, which can be classified into two categories: phantom-base methods and self-calibration methods. Many research groups have explored the phantom-base methods, in which the calibration procedure must be performed before imaging tasks, using a phantom with known geometric information. Some of the phantom-base methods adopt dedicated phantoms consisting of many markers with special patterns [1][2] to acquire all geometric parameters. In such methods, ample markers and precise determination of markers' position are crucial for accurate geometric calibration [3]. However, the precise fabrication is hard to achieve. Therefore, other works have been focused on the calibration methods that use easily accessed phantoms, such as ball bearings without precise arrangement [4]. These methods can acquire part of the geometric parameters.

Different from the phantom-base methods, no phantom study is required before the imaging tasks in self-calibration methods. The geometric parameters are obtained from the imaging objects themselves. Due to the omission of phantom scans, a self-calibration method has some advantages especially in mechanically unstable systems, high-resolution CT, frequently adjusted systems, and many others [5]. However, accurate acquisition of all the geometric parameters with self-calibration method remains a challenge, because no geometric information of imaging object is available. Obviously, if there is a dynamic and variable geometric structure in the system, we need to re-image the phantom to calibrate the system. But in projection base methods, we use the correlation created between the images due to the geometry of the system and obtain the geometric parameters. For this purpose, we have a prior knowledge about the object and using their DRRs<sup>1</sup>, we generate the result with different geometries, based on comparing it with the captured images and measuring their similarity, in this way, we extract the accurate geometry. In our proposed method, it is no longer necessary to have basic information about the object, and we extract the geometry of the system only by having projections.

<sup>1</sup> Digitally Reconstructed Radiograph



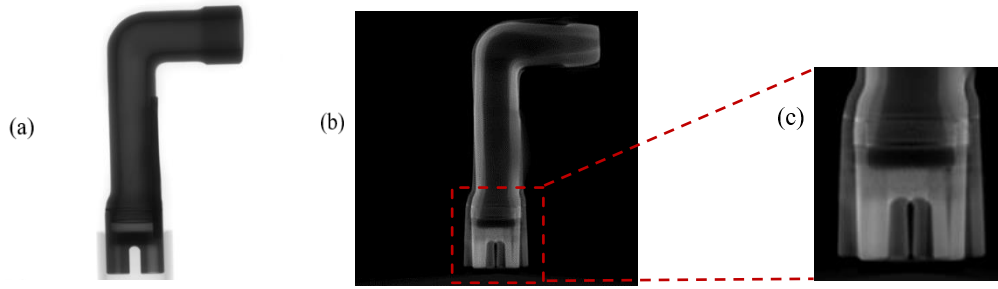


Figure 1: x-ray image of an industrial part (a) and its reconstruction without geometrical calibration (b). the artefacts in the reconstructed object is shown in (c)

In this paper, we propose a new method of geometrical calibration for CT-Scan that measure the misalignment parameters of imaging system by minimizing a geometry-dependent cost function. The cost function is computed from the projections; hence, no prior knowledge of the object shape or positioning is required. There are many geometrical parameters in CT-scan device. Following we propose a method for calibrating most important ones such as transversal and longitudinal and the skew, tilt and slant of the detector.

- Transversal and Longitudinal shift: rigid translation by a vector  $(\delta u, \delta v)^T$  in the  $uv$  reference frame Fig(2-a).
- Tilt: rotation by an angle  $\theta$  about the  $u$  axis Fig(2-b).
- Slant: rotation by an angle  $\eta$  about the  $v$  axis Fig(2-c).
- Skew: rotation by an angle  $\phi$  about the  $y$  axis Fig(2-d).

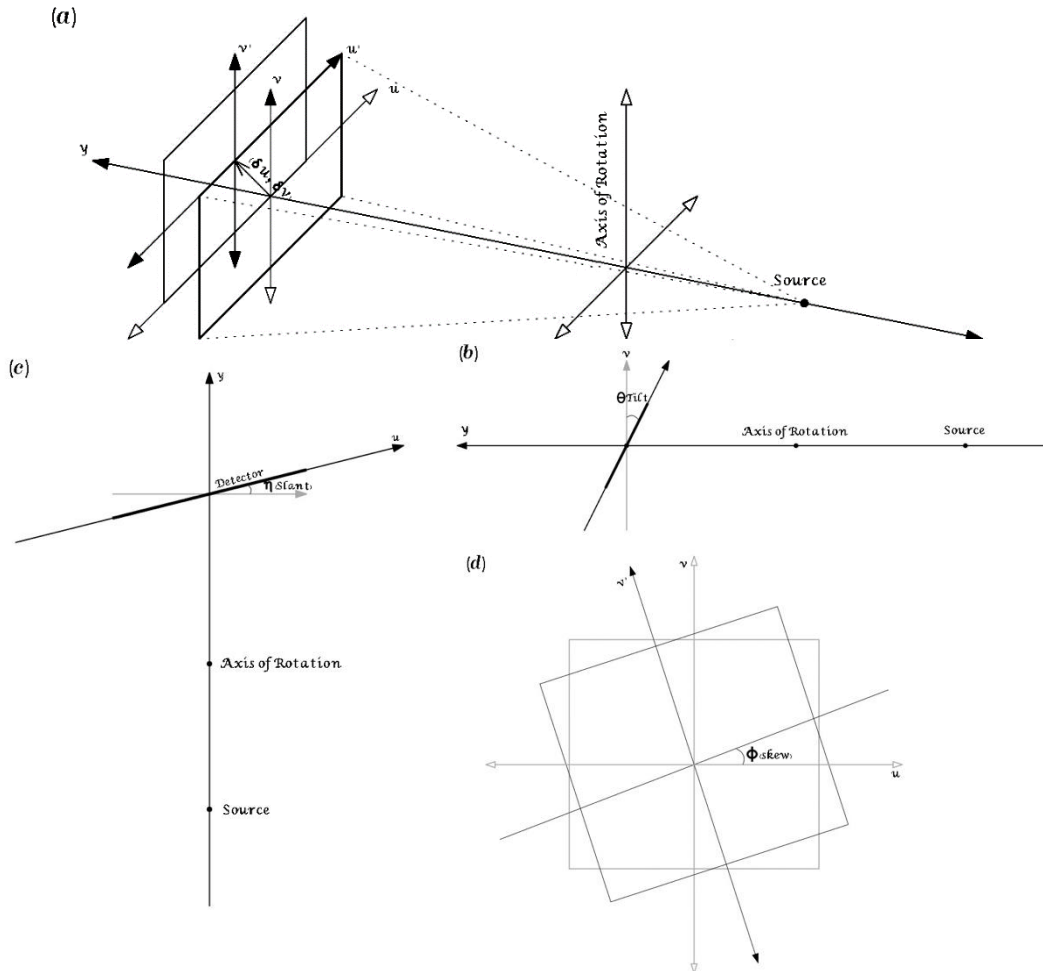


Figure 2: translation by a vector  $(\delta u, \delta v)^T$  in the  $uvw$  detector frame (a). a rotation by an angle  $\theta$  about the  $u$  axis (Tilt) (b). a rotation by an angle  $\eta$  about the  $v$  axis (Slant) (c). a rotation by an angle  $\phi$  about the  $w$  axis (Skew) (d).

## 2 Method

The main idea behind the proposed calibration method is to analyse the projections data, in order to define a cost function that depends on the misalignment parameters. The method begins by reconstructing images from reference images taken with an initial geometry. Although this reconstruction will have many artefacts due to its misaligned geometry, but its DRR is our guide to reaching better geometry. In this way, the model will get closer to the best geometry whenever gets a more similar DRR to the reference images. So, in every single iteration, the model updates the geometry parameters according to the comparing similarity of DRRs with reference images. According to the large search space, it's not beneficial to search randomly, therefore the model updates the parameters corresponding to the gradient descent algorithm. So, the whole process is trying to find the best parameters to maximize the similarity of reference images and DRRs. The process of optimization is shown in Fig (3).

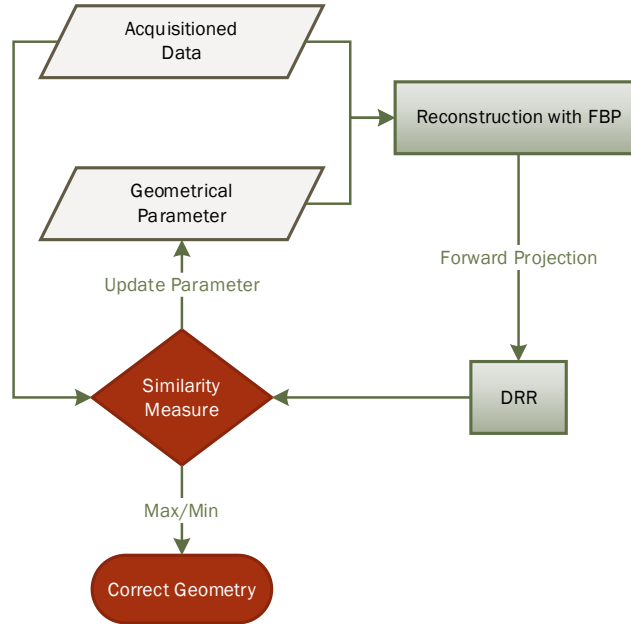


Figure 3 This flowchart demonstrates the iterative procedure of the method.

The performance of our method is strongly dependent on the way that similarity is calculated between DRRs and reference images. Considering its' important role, the models cost function must first have good sensitivity for detecting similarity and secondly have a reasonable computational cost. To ensure we are going through the process correctly, we used the TomoPhantom software package [6], to determine what the best similarity measure might be in our case. the simulator environment utilizes the Shepp-Logan phantom [7] to test similarity measures.

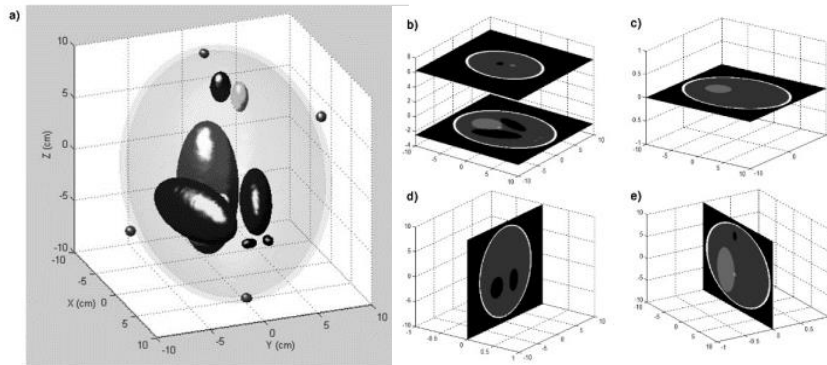


Figure 4 a 3D version of Shepp-Logan phantom (a); axial slices at  $Z = -2.5\text{ cm}$  and  $6.25$  (b); axial slice at  $Z = 0$  (c); coronal slice (d); sagittal slice (e).

On the simulator package, we are able to reconstruct images by a wide range of geometry, although we know the true geometry. In order to compare similarity measures, first we reconstruct the projection given with a wide range of misaligned parameters

(FBP<sup>2</sup>), then we apply the FP<sup>3</sup>s to those misaligned reconstructions to get their projections. Based on both the ideal reconstruction projections and the projection that were given from reconstruction with misaligned parameters, the similarity measure will be calculated. The Fig (5) shows the procedure.

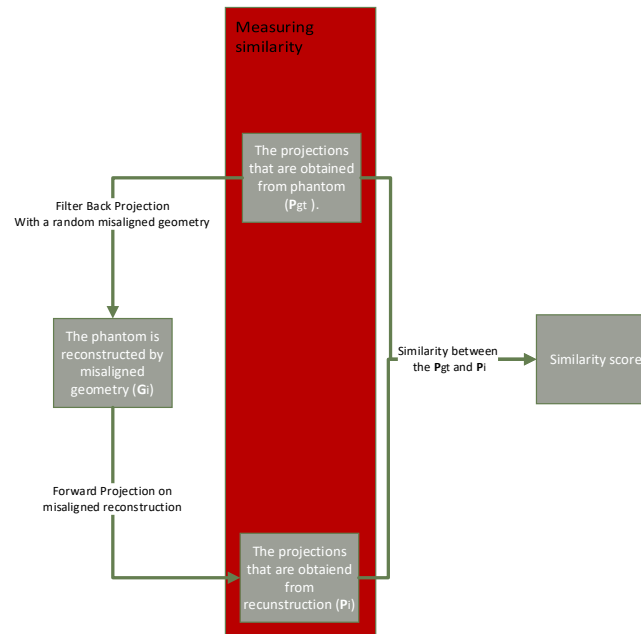


Figure 5 the procedure of calculating similarity scores.

In Table (1) we compared some common similarity measure methods containing different misaligned parameters.

For choosing the best method, a Wide range of similarity measures were examined by giving Intentional misalignment and comparing the corresponding similarity score with the reference images above. As it is shown, in all cases, mutual information has isolated perfectly the optimal point from the rest of the search space. All similarity measures were examined when only one parameter had been misaligned. In Fig (4), the mutual information is shown when all 5 detector parameters ( $\eta$ ,  $\theta$ ,  $\phi$ ,  $u$  and  $v$ ) are misaligned.

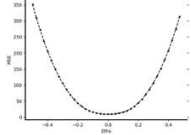
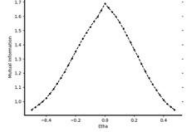
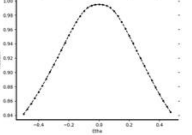
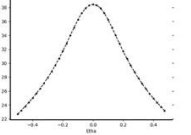
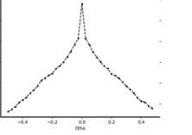
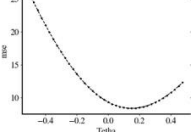
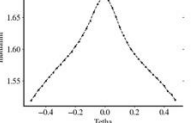
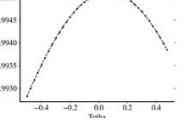
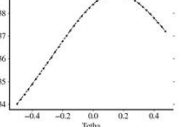
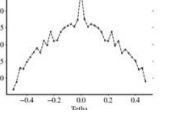
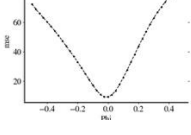
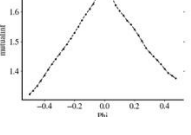
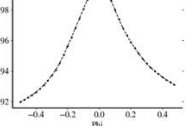
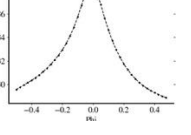
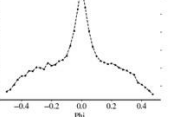
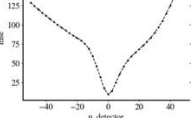
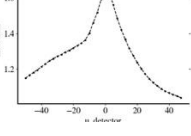
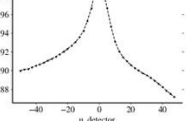
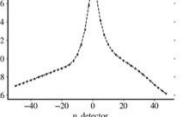
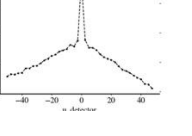
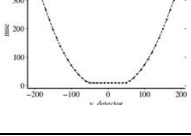
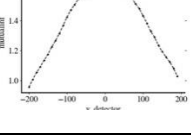
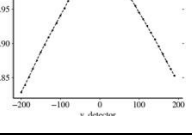
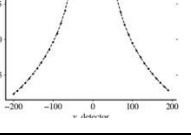
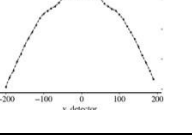
Due to the mutual effects of different misaligned parameters, the optimal point is incorrect and is not well-separated by a single misaligned parameter. Therefore, there is a high probability that the optimization method finds the wrong point as the global optimum geometry. An optimization process that starts with incorrect parameters is highly likely to get involved with the wrong optimum point and produce incorrect results. To overcome these problems, we first try to find which parameter is most sensitive to our cost function, then begin our optimization process with that parameter and update the other parameters accordingly. As you can see in Fig (4), the most effective parameter is  $u$  of detector, so our process starts with  $u$ . The order of parameter updating is  $u \rightarrow \eta \rightarrow \theta \rightarrow v \rightarrow \phi$ .

According to the result of the previous paragraph, we can say that the method searches in different hyperplanes according to its initial point. Hence, it could be claimed if we repeat the optimization process several times, the result will be correct. it means that whenever an optimization algorithm is finished, the initial points obtained from its previous run will be used in the ongoing process. A whole process of optimization is called Sweep. The plot below illustrates how our similarity measure is going to get clearer after every Sweep.

<sup>2</sup> Filter Back Projection

<sup>3</sup> Forward Projection

Table 1: In this table, 5 similarity measures with each geometric parameter have been examined. The time consumption and the well-distinguished optimum point are the 2 most important criteria for choosing the best similarity measure.

	MSE <sup>4</sup>	Mutual-Information <sup>5</sup>	SSIM <sup>6</sup>	PSNR <sup>7</sup>	SCC <sup>8</sup>
Etha					
Theta					
Phi					
U detector					
V detector					
Similarity measure formula (x, y)	$\frac{1}{n} \sum_{i=1}^n (x_i - y_i)^2$ <p>N is the total number of pixels</p>	$I(X; Y) = H(X) - H(X Y)$ <p>H(X) is the entropy for X and H(X Y) is the conditional entropy for X given Y</p>	$\frac{(2\mu_x\mu_y + c_1)}{(\mu_x^2 + \mu_y^2 + c_1)} \times \frac{(2\sigma_{xy} + c_2)}{(\sigma_x^2 + \sigma_y^2 + c_2)}$ <p><math>\mu_x</math>, the pixel sample mean of x  <math>\mu_y</math>, the pixel sample mean of y  <math>\sigma_x^2</math>, the variance of x  <math>\sigma_y^2</math>, the variance of y  <math>\sigma_{xy}</math>, the covariance of x and y  <math>c_1 = (k_1L)^2</math>, <math>c_2 = (k_2L)^2</math>  L, the dynamic range of the pixel-values  <math>k_1=0.01</math> and <math>k_2=0.03</math> by default</p>	$10\log_{10}\left(\frac{R^2}{MSE}\right)$ <p>R is the maximum fluctuation in the input image data type.default is 255</p>	$R_c = x^T W y$ $W = [w_{ij}]_{n \times n}$ $\sum_{i=1}^n \sum_{j=1}^n w_{ij} = 1$ <p>The value of SCC ranged between -1 and 1, with 1 indicating two identical maps while -1 indicating two identical but inverted maps [8]</p>
Avg of computational cost (ms)	0.0011	0.0085	0.3274	0.0014	0.1554

<sup>4</sup> For two pictures A, B you take the square of the difference between every pixel in A and the corresponding pixel in B, sum that up and divide it by the number of pixels.

<sup>5</sup>  $I=mi(A,B)$ , where A and B are equally sized images/signals. Function hist2 (included) is used to determine the joint histogram of the images/signals.

<sup>6</sup> The structural similarity index measure (SSIM) is a method for predicting the perceived quality of digital television and cinematic pictures, as well as other kinds of digital images and videos. SSIM is used for measuring the similarity between two images

<sup>7</sup> Peak signal-to-noise ratio (PSNR) is the ratio between the maximum possible power of an image and the power of corrupting noise that affects the quality of its representation. To estimate the PSNR of an image, it is necessary to compare that image to an ideal clean image with the maximum possible power.

<sup>8</sup> Spatial correlation coefficient shows the correlation between the received average signal gain and the angle of other signal.

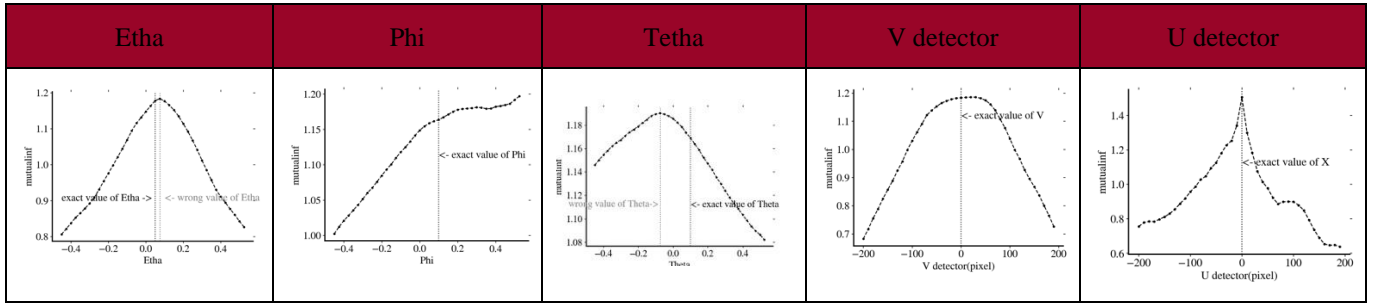


Figure 6 All parameters are misaligned in these plots. Clearly in some parameters like  $\theta$ ,  $\eta$ , and  $v$  the optimum point of mutual information has completely shifted. This problem must be solved in order to get true geometry.

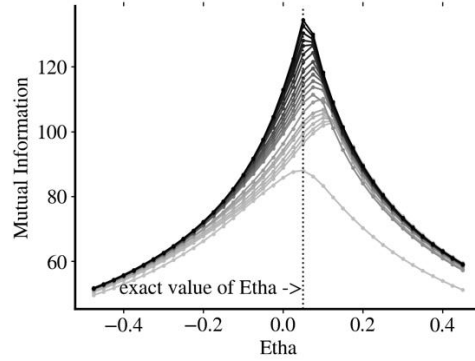
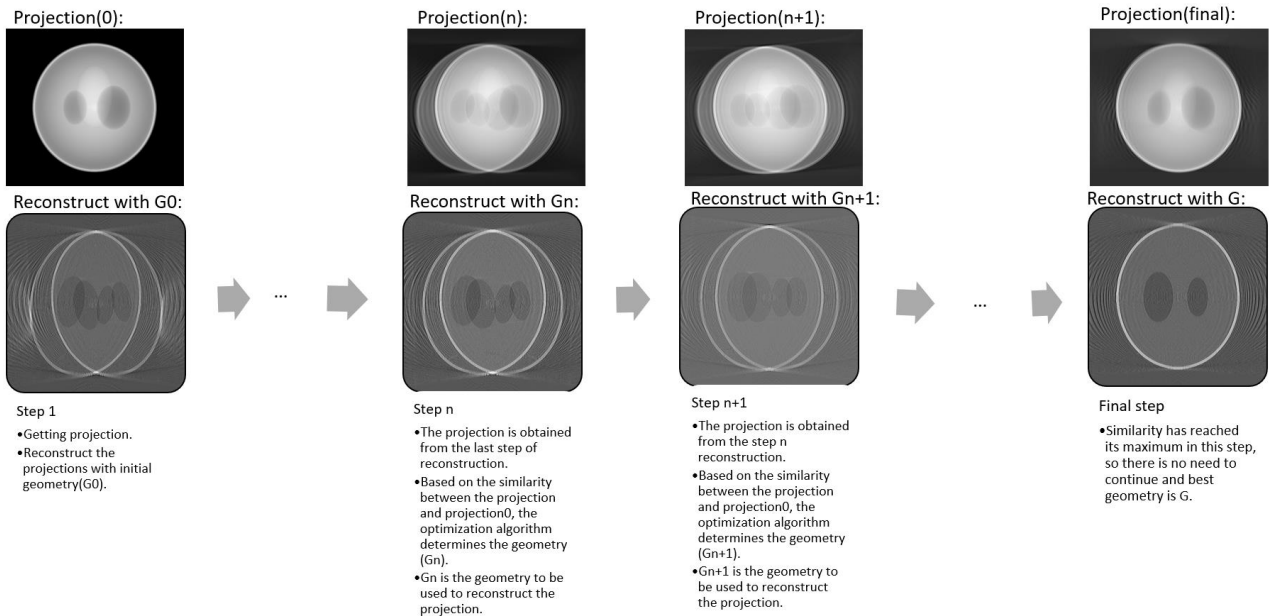


Figure 7 The change in the landscape of mutual information with respect to  $E_{\theta}$  for each sweep is shown. As we can see the extremum of the landscape will approach the correct value after each sweep.

### 3 Result and Discussion

The flow of the Method is presented in Fig (3). we defined the optimization process in which getting DRR plays a central role. The flow graph below illustrates the process by visualizing the result of reconstructions in some steps of optimization in the simulator.





In addition to the simulator job, we applied the method on acquisitioned data using CT-scan system that manufactured by Arman Moj Fanavar company. Table (2) shows the process of updating the parameters after each sweep from the initial parameters to the correct one.

Table 2 The geometry parameters that are estimated by the method in each sweep are written. the reconstruction images are also shown after every sweep, with geometry parameters that are estimated.

First sweep		Second sweep		Final sweep
			...	
$\eta^{\text{rad}}$	0.0000	-0.0156	...	-0.0201
$\theta^{\text{rad}}$	0.0000	0.0124	...	-0.0287
$\varphi^{\text{rad}}$	0.0000	0.0098	...	0.0673
$u^{\text{pixel}}$	0.0000	2.5564	...	6.4027
$v^{\text{pixel}}$	0.0000	15.2489	...	60.8947

The reconstructed image at final state demonstrates the power of our method for geometrical calibration just by acquisitioned data.

## Acknowledgement

We would like to thank Amin Azimi for reading our paper.

## References

- [1] L. Von Smekal, M. Kachelriess, E. Stepina, and W. A. Kalender, "Geometric misalignment and calibration in cone-beam tomography," *Med. Phys.*, vol. 31, no. 12, pp. 3242–3266, 2004.
- [2] Y. B. Cho, D. J. Moseley, J. H. Siewerdsen, and D. A. Jaffray, "Accurate technique for complete geometric calibration of cone-beam computed tomography systems," *Med. Phys.*, vol. 32, no. 4, pp. 968–983, 2005.
- [3] X. H. Li, D. Zhang, and B. Liu, "Sensitivity analysis of a geometric calibration method using projection matrices for digital tomosynthesis systems," *Med. Phys.*, vol. 38, no. 1, pp. 202–209, 2011.
- [4] F. Noo, R. Clackdoyle, C. Mennessier, T. A. White, and T. J. Roney, "Analytic method based on identification of ellipse parameters for scanner calibration in cone-beam tomography," *Phys. Med. Biol.*, vol. 45, no. 11, pp. 3489–3508, 2000.
- [5] Y. Kyriakou, R. M. Lapp, L. Hillebrand, D. Ertel, and W. A. Kalender, "Simultaneous misalignment correction for approximate circular conebeam computed tomography," *Phys. Med. Biol.*, vol. 53, no. 22, pp. 6267–6289, 2008.
- [6] D. Kazantsev, V. Pickalov, S. Nagella, E. Pasca, P. J. Withers, "TomoPhantom, a software package to generate 2D–4D analytical phantoms for CT image reconstruction algorithm benchmarks," *SoftwareX.*, vol. 7, pp.150-155, 2018.
- [7] U. K. Bhowmik, M. Z. Iqbal, R. R. Adhami, "Mitigating motion artifacts in FDK based 3D Cone-beam Brain Imaging System using markers," *Cent. Eur. J. Eng.*, vol. 2, no. 3, pp. 369-382, 2012.
- [8] Y. Chen, "A New Methodology of Spatial Cross-Correlation Analysis," *PLoS ONE*, vol.10, no. 5, 2015.